Diatomite *in situ* Loaded by MOF (ZIF-8) and its Application in Removing Methylene Orange from Aqueous Solutions

Zicheng Chen,[a,b] Huiwen Zhang,[a] Wenlong Luo,[a] Zhibin He,[b] and Lanhe Zhang [a,*]

Diatomite is extensively used as a natural environmental material because of its biogenic origin and stable structure. The zeolitic imidazolate framework (ZIF-8) is a prototypical metal-organic frame (MOF) that is well known for its high surface areas and chemical stability. Herein, a facile method for the generation of diatomite *in situ* loaded by ZIF-8 (D/Z) was reported. The results of powder x-ray diffraction (PXRD) analysis confirmed the successful loading of ZIF-8 on the diatomite. The ZIF-8 were distributed uniformly on the surface of the diatomite from the scanning electron microscope (SEM) images. The specific surface of the D/Z increased due to the loading of the ZIF-8. Methylene orange (MO^-) in an aqueous form was efficiently separated and removed through a simple mixture and filtration process where the D/Z was employed as an absorbent, and the removal rate of the MO^- increased in the case of the sample with more ZIF-8 loaded on the diatomite. In addition, the D/Z was reused after several regenerations by washing out the adsorbed dye.

Keywords: Zeolitic imidazolate framework (ZIF-8); Diatomite; Methylene orange; Filtration

*Contact information: a: School of Chemical Engineering, Northeast Electric Power University, Jilin, Jilin Province 132012, P. R. China; b: Department of Chemical Engineering, University of New Brunswick, Fredericton, NB E3B 5A3, Canada; *Corresponding author: zhanglanhe@163.com*

INTRODUCTION

Metal-organic frameworks (MOFs), also known as a subclass of porous coordination polymers (PCPs) (Zhu and Xu 2014), are synthesized by assembling metal ions with organic ligands (Liu *et al.* 2018). This new class of crystalline porous materials has attracted an immense amount of attention (Zhu and Xu 2014; Zhou *et al.* 2018). The crystal structures of zeolitic imidazolate frameworks (ZIFs), a sub-family of porous metal-organic frameworks (MOFs) (Hu *et al*. 2018), share the same topologies as zeolites, which have high specific surface areas and abundant pores (Pan *et al.* 2011). ZIFs are among the most frequently studied MOFs, due to their excellent chemical and thermal stability (Lee *et al*. 2015; Wang *et al.* 2016), as well as their electrochemical performance (Xu *et al.* 2018). ZIFs have been used in gas storage, separations, catalysis, drug delivery, and chemical sensors (Masingale *et al.* 2009; Stock and Biswas 2012; Liu *et al.* 2014). As a biogenic mineral, diatomite has applications in various fields because of its natural porous structures as well as its stable physical and chemical properties (Chen *et al*. 2017; Zong *et al.* 2018). Diatomite is derived from fossilized remains of diatoms, which are widespread unicellular algae (Medarevic *et al*. 2016; Qi *et al*. 2017); it is found in oceans and fresh waters with its unique highly ordered siliceous cell wall. It is considered to be a green and environmentally friendly material and has been widely used in home wall decoration. Diatomite is also a promising adsorbent substrate due to its natural porous or channel structure and low price (Zong *et al.* 2018).

The conjugation of MOFs with other materials is a good strategy toward the preparation of innovative materials. In particular, MOFs were loaded on the surface of different materials and resulted in film-type MOFs, which improved the applicability of MOFs, especially in separation technology, as catalysts, *etc*. Park and Oh (2017) reported a method for the generation of MOF papers. The resulting MOF papers show an excellent capture ability for methylene orange (MO^-) through a simple filtration process. Also, MOF papers can be reused after the washing process and preserve most of their dye capture ability even they are regenerated several times. Other materials such as pyridine-functionalized graphene, mixed-matrix membranes, and nylon were also used as a building block in the assembly of MOFs for an oxygen reduction reaction (Jahan *et al.* 2012), organic dye separation (Denny and Cohen 2015), and coloration (Yu *et al.* 2016). Metal-organic frameworks and graphite oxide composites could be used for absorbing hydrogen sulfide (Petit *et al*. 2010) and ammonia (Petit and Bandosz 2010), as well as benzene and ethanol (Liu *et al.* 2015). Synthesizing MOFs at carboxy groups on crystalline cellulose nanofibers to separate gas (Matsumoto and Kitaoka 2016) and *in situ* self-assembled Cu414-MOF-based mixed matrix membrane for sensing detecting were also reported (Zhao *et al.* 2016).

MOFs had been successfully used to reactivate the deceased diatoms to prepare an efficient absorbent for carbon dioxide (CO_2) (Liu *et al*. 2014). However, there have been few reports on diatomite as a substrate for MOFs to prepare absorbents of dyes in aqueous media. The pores in the diatomite consist of a vast majority of macro-porous volume and a small quantity of mesopores; thus the specific surface area and meso- and micro-pore volume of the natural diatomite are very poor in comparison to other absorbents such as active carbon and zeolite. In this work, a novel absorbent based on the diatomite was prepared through the conjugation of diatomite with ZIF-8. The absorbent is expected to improve its specific surface area and pore volume *via* forming a hierarchical porous structure in the diatomite. A facile approach of modifying the diatomite by *in situ* loading of the ZIF-8 on it was developed. This composite material was characterized through scanning electron microscopy (SEM), powder x-ray diffraction (PXRD), and a nitrogen adsorption analysis. As an absorbent, the modified diatomite was used to remove an anionic dye, *i.e.* methylene orange in aqueous media (Yakout *et al.* 2019). The dye capture capacity of the absorbent was evaluated by a simple mixing and filtration process.

EXPERIMENTAL

Materials

Methanol was provided by the Tianjin Beichen Fangzheng reagent factory (Tianjin, China). Methylene orange, 2-methylimidazole, and zinc nitrate hexahydrate were purchased from Tianjin Kermel chemical reagent Co., Ltd. (Tianjin, China). Diatomite was provided by the Tianjin Damao chemical reagent factory (Tianjin, China). All the chemicals were not further purified and were used as soon as they were received.

Preparation of ZIF-8

ZIF-8 was prepared according to the reported method (Park and Oh 2017). First, 0.64 g (2.15 mmol) of zinc nitrate hexahydrate ($Zn(NO_3)_2{\cdot}6H_2O$, > 98%) and 0.72 g (8.70 mmol) of 2-methylimidazole ($C_4H_6N_2$, >98%) were dissolved in 50 mL of methanol, respectively. Then the methanol solution containing 2-methylimidazole was slowly

poured into the zinc nitrate hexahydrate solution under stirring. The suspension was kept stirring for 30 min at room temperature and the final product was collected by centrifugation (11000 rpm, 5 min), washed three times with methanol, and dried at 105 °C for 1 h.

Construction of Diatomite *in situ* Loaded by ZIF-8

In a typical procedure, the diatomite (2.00 g, oven-dry weight) was added into 50 ml methanol solution that contained different doses (0.00 g, 0.16 g, 0.32 g, 0.48 g, 0.64 g and 0.80 g) of zinc nitrate hexahydrate while being stirred for 30 min in order to better disperse and adsorb the zinc ions on the surface of the diatomite. Subsequently, another 50 ml of the methanol solution that contained a certain dose (0.00 g, 0.18 g, 0.36 g, 0.54 g, 0.72 g, and 0.90 g, respectively) of 2-methylimidazole was slowly poured into above mixture under stirring and kept stirring for 12 h. Then the mixture was filtered and thoroughly washed by plenty of deionized water. The final product was dried at room temperature in air and denoted as D/Z-0, 1, 2, 3, 4, and 5, respectively.

As shown in Fig. 1, zinc ions were firstly adsorbed on the surface of the diatomite via physical adsorption and then coordinated with silicon hydroxyl groups. When the organic ligands, *i.e.*, 2-methylimidazole were available, the ZIF-8 was constructed and *in situ* loaded on the surface of diatomite.

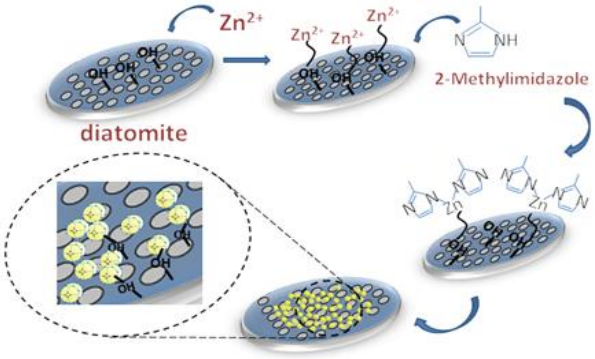

Fig. 1. Preparation of the D/Z composite

Characterization of the Diatomite, ZIF-8 and D/Z

The scanning electron microscope (Hitachi XE-100 + EDAX SEM, Hitachi, Tokyo, Japan) was employed to analyze the morphology of the original diatomite, powder of ZIF-8, and D/Z. The samples were treated with gold spraying before the SEM observation.

The crystalline phase of the samples were characterized by powder x-ray diffraction (PXRD) patterns on a diffractometer (Maxima X XRD-7000, S/L, Shimadzu, Tokyo, Japan) with Cu Kα radiation (λ = 1.5418 Å) at 30 mA, 40 kV, and at a scan rate of 2 °/min with a step size of 0.02°.

Nitrogen adsorption-desorption isotherms were measured at liquid nitrogen temperature (77 K) using a volumetric measured analyzer (Micromeritics, ASAP-2020M, Norcross, GA, USA), and the samples were degassed at 120 °C for 6 h prior to the analysis. The specific surface areas of the samples were calculated using the Brunauer-Emmett-Teller (BET) method, and the Barret-Joyner-Hanlenda (BJH) model was used to determine the pore size.

Capture of Methylene Orange Dye

The capture of the MO^- in aqueous solution was evaluated through a simple filtration process. The MO^- dye was dissolved in deionized water with a concentration of 5 ppm and filtrated for further use. D/Z (0.5 g, oven-dry weight) was added into the aqueous solution of the MO^- (5 ppm, 12 mL) and stirred for 1 min. Then the mixture was slowly poured into a conical glass funnel with a filter paper, where the filtrate was collected for absorbance analysis with a UV-vis spectrophotometer at 462 nm. The removal rate of the MO^- dye was calculated through the following formula and reported as an average removal rate of three tests,

$$R = \frac{A_1 - A_0}{A_1} \times 100\% \quad (1)$$

where the R is the removal rate, and A_1 and A_0 are the absorbance of the control MO^- aqueous solution (5 ppm) and the filtrate, respectively.

The experiment process is illustrated in Fig. 2 below.

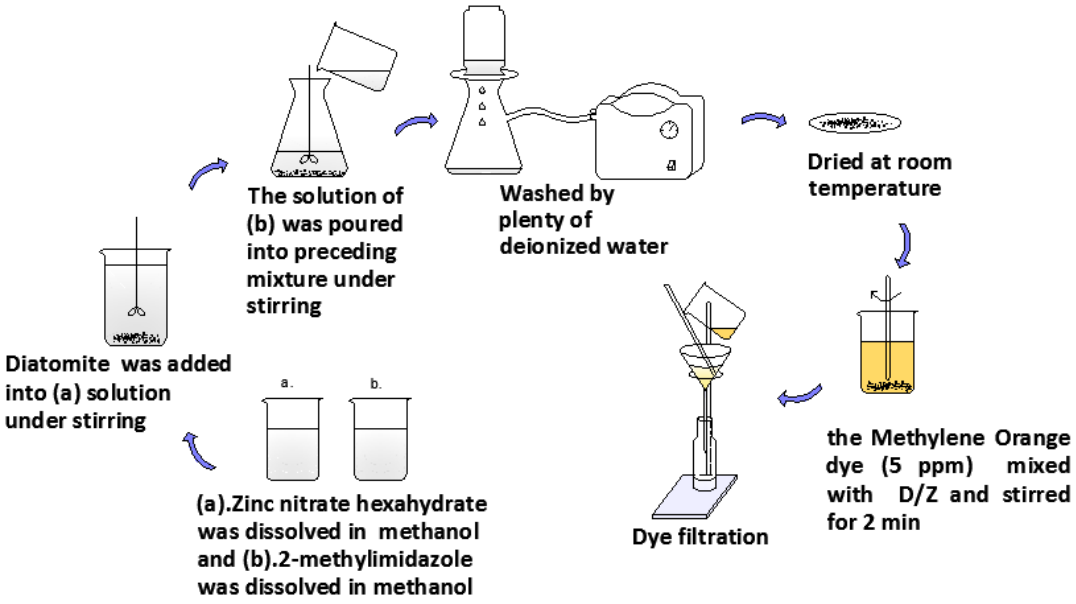

Fig. 2. Experimental procedure

The Reuse of D/Z

The D/Z absorbed with MO^- was washed thoroughly with methanol and then was dried at 65 °C for another filtration process.

RESULTS AND DISCUSSION

The Diatomite *in situ* Loaded by ZIF-8

As shown in Fig. 3, the synthesized ZIF-8 matched the corresponding simulated patterns, and the results of the PXRD analysis confirmed the formation of ZIF-8 (Hu *et al*. 2018). The PXRD pattern of the diatomite sample shows broad peaks at 2θ = 22.0° and 36.1° (Fig. 3) respectively, suggesting that the amorphous phase of the SiO_2 is present in the diatomite. The characteristic peaks of the ZIF-8 were also observed in the

pattern of D/Z-4, which confirmed that the ZIF-8 was successfully *in situ* loaded onto the diatomite.

In the scanning electron microscopy (SEM) images, a mass of regular rhombic morphology of the ZIF-8 can be observed clearly with a particle size of approximately ten nanometers. (Fig. 4a). Through the *in situ* loading of ZIF-8, nano-sized ZIF-8 particles were compactly and uniformly coated on the surface and sides of the disc of diatomite (Fig. 4e-g). Compared with the diatomite *in situ* loaded by ZIF-8, the surface of the control diatomite was neat with distinct pore channels. (Fig. 4b-d). Due to the *in situ* loading of the ZIF-8 on the surface of the diatomite, the size of macropores in the diatomite became smaller in comparison to the control diatomite. The new mesopores could generate between the nanoparticles of ZIF-8 or between ZIF-8 and the macropores in the diatomite. A hierarchical pore system was constructed on the surface of the diatomite that was *in situ* loaded by ZIF-8, which was expected to improve the performance of D/Z as a dye absorbent. The results in Fig. 4 confirmed again the formation of ZIF-8 and its successful *in situ* loading on the surface of the diatomite.

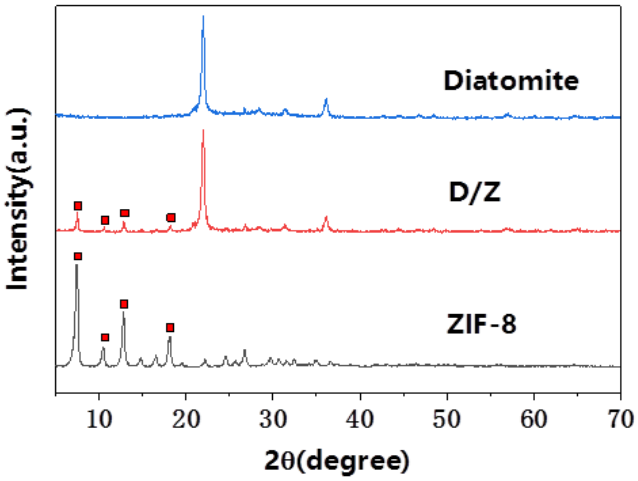

Fig. 3. PXRD patterns of diatomite, D/Z, and ZIF-8

As shown in Fig. 5a, the pore structure in the diatomite was irregular and the pore size seemed uneven, which is given by the jump point. The N_2 adsorption-desorption isotherms of ZIF-8 (Fig. 5b) combined type I and II isotherms with a hysteresis loop that indicated the mesoporous formed between the nanoparticles. The specific surface area of the ZIF-8 reached 1430 m^2/g, which is much higher than the diatomite (5.3 m^2/g). As for the D/Z-4 (Fig. 5c), slit pores may exist in the composite on account of the grain packing, which suggests that the ZIF-8 was loaded on the diatomite and the hierarchical pore structure has been constructed. It is noteworthy that the specific surface area of the D/Z-4 increased to 35.3 m^2/g, which is significantly higher than that of the control diatomite because of the loading of ZIF-8.

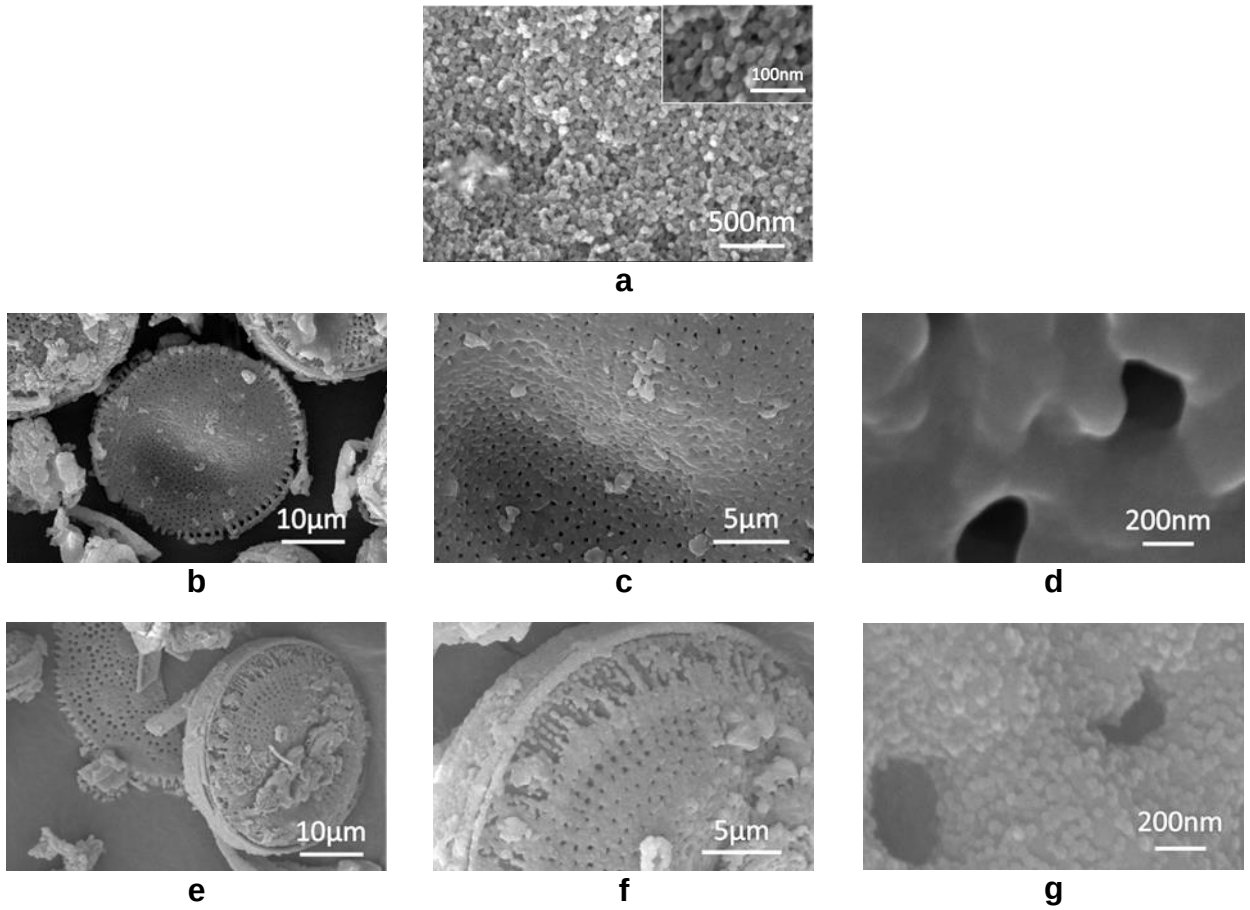

Fig. 4. SEM images (a): ZIF-8 particles; (b, c, d): The control diatomite; (e, f, g): The diatomite *in situ* loaded by ZIF-8 particles

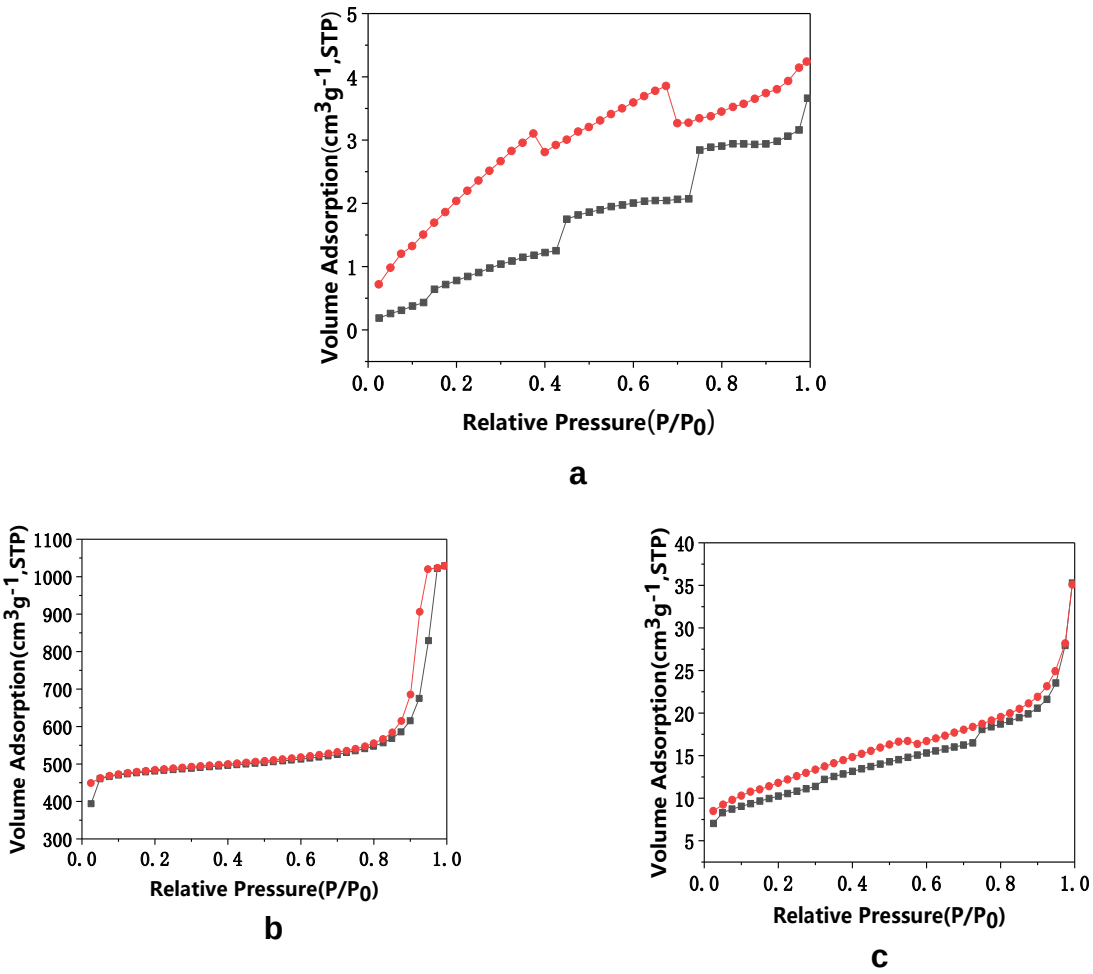

Fig. 5. N_2 adsorption-desorption isotherms (a); the control diatomite; (b) ZIF-8; (c) D/Z-4

Capture of the Methylene Orange Dye

Because ZIF-8 particles have a positive surface charge (Park and Oh 2017), the anionic organic dyes can be captured through an electrostatic interaction by taking advantage of the positive surface charge of the ZIF-8. As shown in Fig .6a, the dye capture ability gradually increased from D/Z-0 to D/Z-5. In particular, the dye removal rate in the case of D/Z-4 and D/Z-5 reached 94.74% and 95.67%, respectively. Obviously, the control diatomite had almost no dye adsorption capacity and the more ZIF-8 loaded on the diatomite, the better the dye capture capacity was observed in the D/Z. The dye removal ability of D/Z-4 and D/Z-5 was quite close. Compared with D/Z-4 and D/Z-5, the dye removal ability of D/Z-3 was weak and D/Z-1 and 2 were only a bit better than the control diatomite. It could be supposed that the dose of ZIF-8 loaded on the diatomite was important to the dye capture capacity of D/Z.

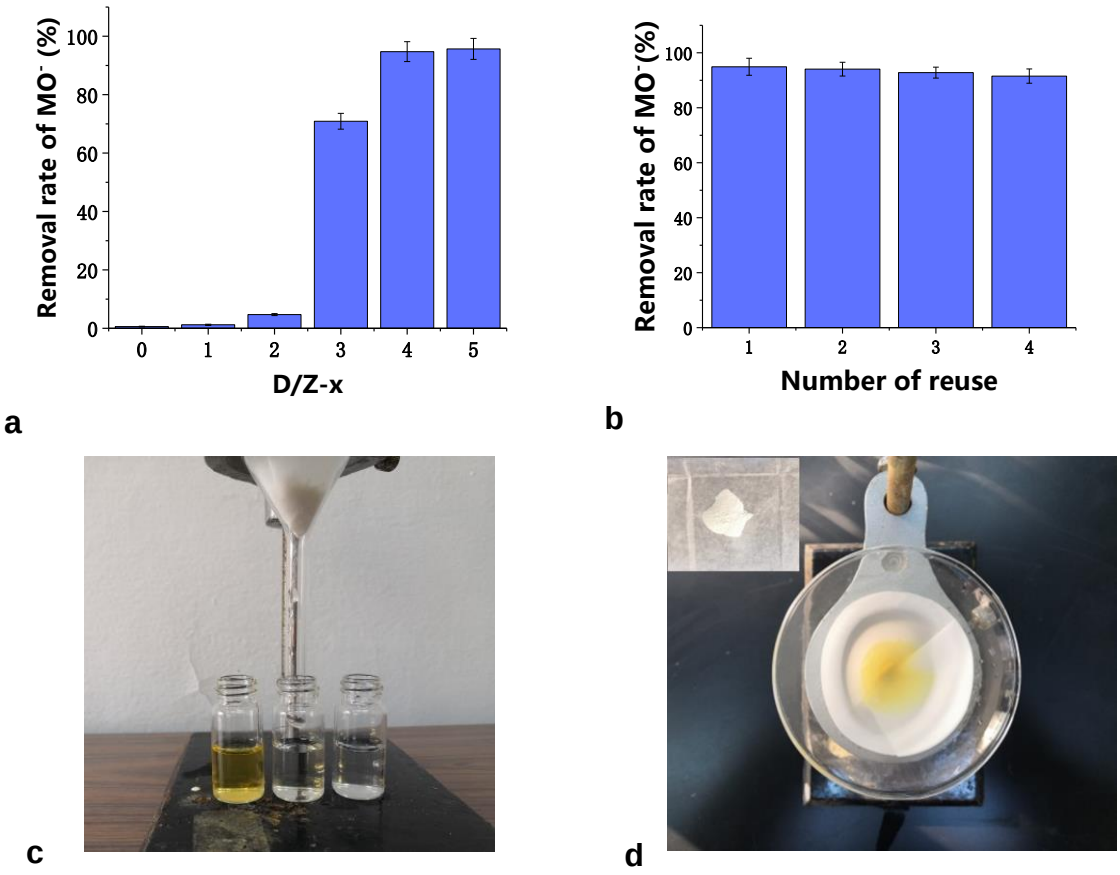

Fig. 6. The capture and removing of MO^- in aqueous media via a filtration process; (a): The removal rate of MO^- in the case of different D/Z (x=0,1, 2, 3, 4, 5); (b): The removal rate of MO^- when the regenerated D/Z-4 was used; (c): The filtrate of MO^- aqueous solution (the middle one), the control MO^- aqueous solution (the left one), and the deionized water (the right one); (d): D/Z-4 absorbed by MO^- (the yellow one) and D/Z-4 before filtration (the white one)

As shown in Fig. 6c, the filtrate of the dye aqueous solution became nearly as colorless as the deionized water after the solution suffered from the above mixing and filtration process by D/Z-4. The color of D/Z-4 was different before and after the mixture and filtration process. Because almost all of the MO^- dye in solution was captured, the D/Z-4 changed from grey-white to light yellow as shown in Fig. 6d. According to the results in Fig. 6, D/Z-4 is an effective dye absorbent. As an absorbent, its recyclability is very important considering its further application. It was found that D/Z-4 could be reused after regeneration *via* a washing process, and its excellent dye capture ability was preserved even after recycling it four times (Fig. 6b). Based on these results, the absorbent (D/Z-4) can potentially be used in circumstances where other anionic dyes or some anionic pollutants such as phosphates are present in aqueous systems. In this sense, comprehensive work is highly needed to unlock such possibilities.

CONCLUSIONS

1. Diatomite *in situ* loaded by ZIF-8 (D/Z) was successfully constructed through a facile

process. The SEM images and nitrogen adsorption-desorption isotherms of D/Z-4 demonstrated that a hierarchical pores structure of D/Z-4 was constructed and D/Z-4 had the smaller average pore size and better specific surface area when compared with the natural diatomite.

2. Methylene orange dye in aqueous solution can be efficiently separated and removed *via* a rapid mixture and filtration process with D/Z-4 as an absorbent, where the removal rate of MO^- reached 94.7%. It was also found that D/Z-4 could be regenerated and reused, and its MO^- dye capturing ability was largely preserved even after four cycles of reuse.

ACKNOWLEDGMENTS

The authors would like to acknowledge support from Science and Technology Development Plan of Jilin Province of P.R.C. (No. 20190303065SF).

REFERENCES CITED

Chen, Y., Wu, Q., Zhou, C., and Jin, Q. (2017). "Enhanced photocatalytic activity of La and N co-doped TiO_2/diatomite composite," *Powder Technology* 322, 296-300. DOI: 10.1016/j.powtec.2017.09.026

Denny, M. S., and Cohen, S. M. (2015). "*In situ* modification of metal-organic frameworks in mixed-matrix membranes," *Angewandte Chemie International Edition* 54(31), 9029-9032. DOI: 10.1002/anie.201504077

Hu, L., Chen, L., Fang, Y., Wang, A., Chen, C., and Yan, Z. (2018). "Facile synthesis of zeolitic imidazolate framework-8 (ZIF-8) by forming imidazole-based deep eutectic solvent," *Microporous and Mesoporous Materials* 268(15), 207-215. DOI: 10.1016/j.micromeso.2018.04.039

Jahan, M., Bao, Q., and Loh, K. P. (2012). "Electrocatalytically active graphene–porphyrin MOF composite for oxygen reduction reaction," *Journal of the American Chemical Society* 134(15), 6707-6713. DOI: 10.1021/ja211433h

Lee, Y.-R., Jang, M.-S., Cho, H.-Y., Kwon, H.-J., Kim, S., and Ahn, W.-S. (2015). "ZIF-8: A comparison of synthesis methods," *Chemical Engineering Journal* 271(1), 276-280. DOI: 10.1016/j.cej.2015.02.094

Liu, D., Gu, J., Liu, Q., Tan, Y., Li, Z., Zhang, W., Su, Y., Li, W., Cui, A., Gu, C., and Zhang, D. (2014). "Metal-organic frameworks reactivate deceased diatoms to be efficient CO_2 absorbents," *Advanced Materials* 26(8), 1229-1234. DOI: 10.1002/adma.201304284

Liu, G. Q., Wan, M. X., Huang, Z. H., and Kang, F. (2015). "Preparation of graphene/ metal-organic composites and their adsorption performance for benzene and ethanol," *New Carbon Materials* 30(6), 566-571. DOI: 10.1016/S1872-5805(15)60205-0

Liu, X., Tang, B., Long, J., Zhang, W., Liu, X., and Mirza, Z. (2018). "The development of MOFs-based nanomaterials in heterogeneous organocatalysis," *Science Bulletin* 63(8), 502-524. DOI: 10.1016/j.scib.2018.03.009

Petit, C., and Bandosz, T. J. (2010). "Enhanced adsorption of ammonia on metal-organic framework/graphite oxide composites: Analysis of surface interactions," *Advanced Functional Materials* 20(1), 111-118. DOI: 10.1002/adfm.200900880

Petit, C., Mendoza, B., and Bandosz, T. J. (2010). "Hydrogen sulfide adsorption on MOFs and MOF/graphite oxide composites," *ChemPhysChem* 11(17), 3678-3684. DOI: 10.1002/cphc.201000689

Masingale, M. P., Alves, E. F., Korbieh, T. N., Bose, S. K., and Francis, R. C. (2009). "An oxidant to replace nitrobenzene in lignin analysis," *BioResources* 4(3), 1139-1146. 1139-1146. DOI: 10.1007/s00226-008-0200-y

Matsumoto, M., and Kitaoka, T. (2016). "Ultraselective gas separation by nanoporous metal-organic frameworks embedded in gas-barrier nanocellulose films," *Advanced Materials* 28(9), 1765-1769. DOI: 10.1002/adma.201504784

Medarevic, D., Losic, D., and Ibric, S. (2016). "Diatoms - nature materials with great potential for bioapplications," *Hemijska Industrija* 70(6), 613-627. DOI: 10.2298/HEMIND150708069M

Pan, Y., Liu, Y., Zeng, G., Zhao, L., and Lai, Z. (2011). "Rapid synthesis of zeolitic imidazolate framework-8 (ZIF-8) nanocrystals in an aqueous system," *Chemical Communications* 47(7), 2071. DOI: 10.1039/c0cc05002d

Park, J., and Oh, M. (2017). "Construction of flexible metal–organic framework (MOF) papers through MOF growth on filter paper and their selective dye capture," *Nanoscale* 9(35), 12850-12854. DOI: 10.1039/C7NR04113F

Qi, Y., Wang, X., and Cheng, J. J. (2017). "Preparation and characteristics of biosilica derived from marine diatom biomass of *Nitzschia closterium* and *Thalassiosira*," *Chinese Journal of Oceanology and Limnology* 35(3), 668-680. DOI: 10.1007/s00343-017-5329-9

Stock, N., and Biswas, S. (2012). "Synthesis of metal-organic frameworks (MOFs): Routes to various MOF topologies, morphologies, and composites," *Chemical Reviews* 112(2), 933-969. DOI: 10.1021/cr200304e

Wang, X.-W., Yan, T., Wan, J., Zhao, L.-F., and Tu, Y. (2016). "Zeolitic imidazolate framework-8 as a nanoadsorbent for radon capture," *Nuclear Science and Techniques* 27(1), 2-7. DOI: 10.1007/s41365-016-0008-7

Xu, X., Qi, C., Hao, Z., Wang, H., Jiu, J., Liu, J., Yan, H., and Suganuma, K. (2018). "The surface coating of commercial $LiFePO_4$ by utilizing ZIF-8 for high electrochemical performance lithium ion battery," *Nano-Micro Letters* 10(1), 1. DOI: 10.1007/s40820-017-0154-4

Yakout, S. M., Hassan, M. R., El-Zaidy, M. E., Shair, O. H., and Salih, A. M. (2019). "Kinetic study of methyl orange adsorption on activated carbon derived from pine (*Pinus strobus*) sawdust," *BioResources* 14(2), 4560-4574. DOI: 10.15376/biores.14.2.4560-4574

Yu, M., Li, W., Wang, Z., Zhang, B., Ma, H., Li, L., and Li, J. (2016). "Covalent immobilization of metal–organic frameworks onto the surface of nylon—A new approach to the functionalization and coloration of textiles," *Scientific Reports* 6(1), 22796. DOI: 10.1038/srep22796

Zhao, C., Ma, J., and Liu, Q. (2016). "An in situ self-assembled Cu_4I_4–MOF-based mixed matrix membrane: A highly sensitive and selective naked-eye sensor for gaseous HCl," *Chemical Communications* 52(30), 5238-5241. DOI: 10.1039/C6CC00189K

Zhou, N., Du, Y., Wang, C., and Chen, R. (2018). "Facile synthesis of hierarchically porous carbons by controlling the initial oxygen concentration *in situ* carbonization of

ZIF-8 for efficient water treatment," *Chinese Journal of Chemical Engineering* 26(12), 2523-2530. DOI: 10.1016/j.cjche.2018.05.014

Zhu, Q. L., and Xu, Q. (2014). "Metal–organic framework composites," *Chem. Soc. Rev.* 43(16), 5468-5512. DOI: 10.1039/c3cs60472a

Zong, P., Makino, D., Pan, W., Yin, S., Sun, C., Zhang, P., Wan, C., and Koumoto, K. (2018). "Converting natural diatomite into nanoporous silicon for eco-friendly thermoelectric energy conversion," *Materials & Design* 154(15), 246-253. DOI: 10.1016/j.matdes.2018.05.042

Article submitted: July 8, 2019; Peer review completed: October 26, 2019; Revised version received: November 2, 2019; Accepted: November 11, 2019; Published: November 13, 2019.
DOI: 10.15376/biores.15.1.265-275